

Particle Simulation of Potential Formation due to Local ECR along Diverging Magnetic-Field Lines

ISHIMORI Takayuki, KANEKO Toshiro*, ISHIGURO Seiji¹, HATAKEYAMA Rikizo and SATO Noriyoshi

Graduate School of Engineering, Tohoku University, Sendai 980-8579, Japan

¹*National Institute for Fusion Science, Toki 509-5292, Japan*

(Received: 5 December 2000 / Accepted: 27 August 2001)

Abstract

Plasma potential formation due to local electron cyclotron resonance (ECR) along diverging magnetic-field lines is investigated by using a two-and-a-half dimensional particle simulation. When an electromagnetic wave for ECR is applied to a plasma flow, a potential drop in the downstream region from the ECR point is enhanced. In the case of the small wave amplitude, the potential structure is formed based on an ambipolar mechanism. In the case of the large wave amplitude, on the other hand, trapped electrons in the downstream region induce a further increase in the potential drop superimposed on the ambipolar potential.

Keywords:

local electron cyclotron resonance, diverging magnetic-field lines, particle simulation, ambipolar plasma potential, trapped electrons

1. Introduction

Plasma potential formation along diverging magnetic-field lines is an important subject concerning plasma thrust by expansion in a magnetic nozzle [1], ion impinging in reactive plasma processing [2,3], ion conic generation in the ionosphere [4], and thermal flow to a divertor region in a fusion oriented plasma [5]. As for the potential formation in a laboratory experiment using an electron cyclotron resonance (ECR) discharge plasma source, it is reported that the potential profile is similar to the field profile of a diverging magnetic-field configuration [6]. Since an electron pitch angle is larger than ion's even at the entrance of the diverging configuration in such a plasma, a charge separation takes place at the magnetic gradient region, resulting in the potential decrease toward the downstream region in order to cancel this charge separation. When ECR locally occurs at a magnetic gradient region, the charge separation is expected to be more enhanced because of a

strong increase in the electron pitch angle.

On the other hand we have qualitatively demonstrated the potential formation due to local ECR at a magnetic gradient region in basic experiments with a Q-machine plasma apparatus, where a large potential drop is observed in the downstream region from the ECR point [7]. It is also shown that the potential formation is closely related to electron and ion energies parallel to the magnetic field after the ECR heating and that ions are accelerated up to the value equivalent to the potential drop. However, this experimental work is limited to a phenomenological investigation and the quantitative dependence of potential structure on plasma parameters is not clarified. Concerning a particle simulation on this problem, the relationship between the potential and the plasma parameters was investigated by Hooper [8]. In this simulation, however, the electron heating is artificially realized by changing the

*Corresponding author's e-mail: kaneko@ecei.tohoku.ac.jp

perpendicular energy distribution function at the ECR point in the absence of an electromagnetic wave propagation. Thus, the correlation between the wave heating and the potential structure has not been known. Therefore, in order to clarify the above-mentioned points in the fashion of quantitative analysis, we investigate the dependence of the potential structure on the wave amplitude and the time evolution of spatial potential-profile through a two-and-a-half dimensional particle simulation which realizes local ECR by externally applying an electromagnetic wave.

2. Simulation Model

We employ a two-and-a-half dimensional electrostatic particle simulation code on magnetized plasmas. Our simulation code applies the standard particle-in-cell (PIC) method [9], which follows particle motions in a self-consistent electric field generated by particles and an external stationary magnetic field. A simulation system with magnetic-field lines is schematically shown in Fig. 1. Plasma particles are assumed to be emitted at $x = L_x$ and $y = 0.4L_y \sim 0.6L_y$ from a plasma reservoir with electron and ion densities n_S and temperatures T_S . A floating collector is placed at $x = 0$ and $y = 0 \sim L_y$. The simulation system is initially empty and a particle injection with a constant rate starts at $t = 0$ from the emitter. The boundaries at $x = L_x$, $y = 0$, and $y = L_y$ are grounded while the collector ($x = 0$) potential is floated. These conditions correspond to the Q-machine experimental configuration. An external static magnetic field B is shown in Fig. 2(a) and a degree of magnetic divergence R_m^{-1} is defined as the reciprocal of mirror ratio R_m which is the ratio of B at $x = L_x$ to that at $x = 0$. An externally-applied electromagnetic wave with right-hand circular polarization propagates toward the emitter and the wave amplitude E_μ is assumed to be spatially constant under

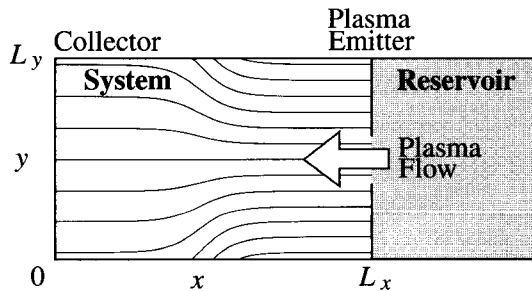


Fig. 1 Schematic of simulation system and diverging magnetic-field line.

the condition of the low density plasma.

Simulation parameters used in this paper are as follows. The ion to electron mass ratio m_i/m_e is fixed at 400. The ratio of the electron cyclotron to electron plasma frequency is $\omega_{ce}/\omega_{peS} = 5$, and the ratio of the applied electromagnetic wave to electron cyclotron frequency is $\omega/\omega_{ceS} = 0.9$. The normalized wave amplitude $\hat{E}_\mu (\equiv E_\mu/(T_{eS}/e\lambda_{DeS}))$ is changed from 0 to 1.2. Here, T_{eS} and λ_{DeS} are the electron temperature and the Debye length, respectively. The time step width Δt is $0.02\omega_{peS}^{-1}$. The system sizes L_x and L_y are $512\lambda_{DeS}$ and $128\lambda_{DeS}$, respectively. The subscript "S" stands for the parameters in the reservoir.

3. Simulation Results

A typical example of the plasma potential $e\phi/T_{eS}$ at $y/\lambda_{DeS} = 64$ in the steady state ($\omega_{peS}t = 3000$) with $R_m^{-1} = 2.0$ is presented in Fig. 2(b), where an arrow at $x/\lambda_{DeS} = 291$ indicates the position of the ECR point. For $\hat{E}_\mu = 0.0$ (dotted line), the potential decreases slightly toward the collector along the magnetic-field lines and its profile is similar to that of the magnetic-field strength. For $\hat{E}_\mu = 0.2$ (solid line), on the other hand, the potential decreases strongly in the downstream region from the ECR point. The electrons are accelerated by the ECR in the direction perpendicular to the magnetic field and accelerated in the axial direction by $-\mu\nabla_{\parallel}B$ force, while the ions are not directly affected by the ECR. Thus, the potential drop which decelerates electrons and accelerates ions is expected to be formed in the downstream region under the quasi-neutrality condition

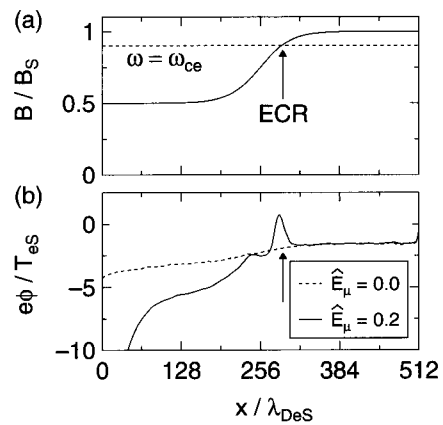


Fig. 2 Spatial profiles of (a) magnetic field strength and (b) plasma potential $e\phi/T_{eS}$ at $y/\lambda_{DeS} = 64$ with $R_m^{-1} = 2.0$ for $\hat{E}_\mu = 0.0$ (dotted lines) and 0.2 (solid lines) at $\omega_{peS}t = 3000$.

(μ : magnetic moment). Here, a potential peak is also observed around the ECR point. Since the only electrons are accelerated by the ECR in the axial direction as described above, the ions are left around the ECR point. Thus, the ion rich condition is realized and the potential peak is expected to be formed there.

Since the potential drop $|e\phi/T_{eS}|$, which is the potential difference between the emitter and the downstream region ($x/\lambda_{DeS} = 128$), is considered to decelerate and reflect the electrons so as to satisfy the quasi-neutrality condition in the downstream region, $|e\phi/T_{eS}|$ is expected to be related to an average electron energy parallel to the magnetic-field lines $\varepsilon_{e\parallel}/T_{eS}$ and result in accelerating ions up to the same energy of the electrons. In order to clarify the relation between them, $|e\phi/T_{eS}|$ and $\varepsilon_{e\parallel}/T_{eS}$ in the steady state ($\omega_{peS}t = 3000 \sim 4000$) are plotted as a function of \hat{E}_μ with $R_m^{-1} = 2.0$ at $x/\lambda_{DeS} = 128$, as given in Fig. 3. $|e\phi/T_{eS}|$ increases with an increase in \hat{E}_μ , being followed by a gradual saturation for $\hat{E}_\mu \geq 0.8$. On the other hand, $\varepsilon_{e\parallel}/T_{eS}$ increases in the same way as $|e\phi/T_{eS}|$, but gradually decreases for $\hat{E}_\mu \geq 0.4$. The decrease in $\varepsilon_{e\parallel}/T_{eS}$ seems to be related to the efficiency in an energy transfer from the wave to electrons at the ECR point. Then, we measure average electron energies parallel $\varepsilon_{e\parallel}/T_{eS}$ and perpendicular $\varepsilon_{e\perp}/T_{eS}$ to the magnetic-field lines at ECR point in the steady state. As a result, it is found that the passing time of electrons in the ECR region becomes shorter due to increased $\varepsilon_{e\parallel}/T_{eS}$, and thus $\varepsilon_{e\perp}/T_{eS}$ does not increase even if \hat{E}_μ is increased. Therefore, the saturation of the total energy $\varepsilon_{cr}/T_{eS} (= \varepsilon_{e\parallel}/T_{eS} + \varepsilon_{e\perp}/T_{eS})$ at the ECR

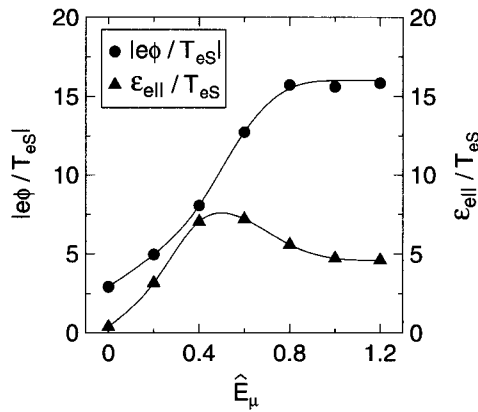


Fig. 3 The absolute value of potential drop $|e\phi/T_{eS}|$ (closed circles) and the average electron energy parallel to the magnetic field $\varepsilon_{e\parallel}/T_{eS}$ (closed triangles) at $x/\lambda_{DeS} = 128$ as a function of \hat{E}_μ with $R_m^{-1} = 2.0$ in steady state.

point is considered to cause the saturation of $\varepsilon_{e\parallel}/T_{eS}$ in the downstream region. Furthermore, since the electrons are decelerated by $|e\phi/T_{eS}|$ which increases even for $\hat{E}_\mu \geq 0.4$, $\varepsilon_{e\parallel}/T_{eS}$ in the downstream region is considered to decrease gradually for $\hat{E}_\mu \geq 0.4$.

In order to investigate the difference of $|e\phi/T_{eS}|$ and $\varepsilon_{e\parallel}/T_{eS}$ dependences on larger \hat{E}_μ as shown in Fig. 3 in detail, temporal evolutions of $|e\phi/T_{eS}|$, electron density n_e , and ion density n_i in the downstream region ($x/\lambda_{DeS} = 128$) with $R_m^{-1} = 2.0$ for $\hat{E}_\mu = 0.2$ and 0.8 are presented in Figs. 4 and 5, respectively. In both the cases of $\hat{E}_\mu = 0.2$ and 0.8, $|e\phi/T_{eS}|$ increases as time goes by in the same way, but the time when the potential attains to the maximum and its value are different. In the case of $\hat{E}_\mu = 0.2$, $|e\phi/T_{eS}|$ starts to apparently increase at $\omega_{peS}t = 1200$, saturates after attaining to the maximum value at $\omega_{peS}t = 1500$, and the local maximum value is observed only once. The time of $\omega_{peS}t = 1200$ corresponds to the time when n_e starts to increase in the downstream region as shown in Fig. 4(b). The other time of $\omega_{peS}t = 1500$ corresponds to the time when n_i starts to increase, which means that the plasma flow arrives at the observation point ($x/\lambda_{DeS} = 128$). In the case of $\hat{E}_\mu = 0.8$, on the other hand, $|e\phi/T_{eS}|$ increases not only at $\omega_{peS}t = 1200$, which is the same as in the case of $\hat{E}_\mu = 0.2$, but also at $\omega_{peS}t = 2200$, attaining to the maximum value just after the second increase. Furthermore, the times of the first and the second increases in $|e\phi/T_{eS}|$ correspond to the times of the first and second increases in n_e , respectively. These second increases in $|e\phi/T_{eS}|$ and n_e are observed in the time scale when the plasma flow arrives at the collector, which will be discussed in Section 4 in

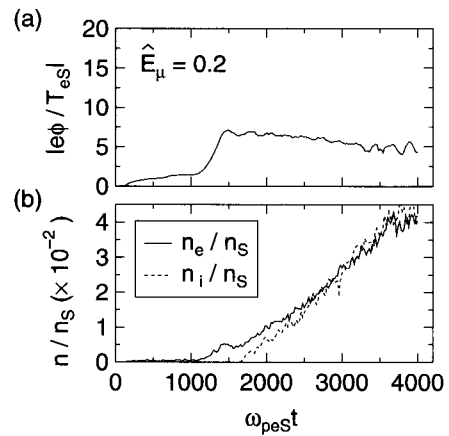


Fig. 4 Temporal evolutions of (a) the absolute value of potential drop $|e\phi/T_{eS}|$ and (b) the density n/n_S at $x/\lambda_{DeS} = 128$, $y/\lambda_{DeS} = 64$ with $R_m^{-1} = 2.0$ for $\hat{E}_\mu = 0.2$.

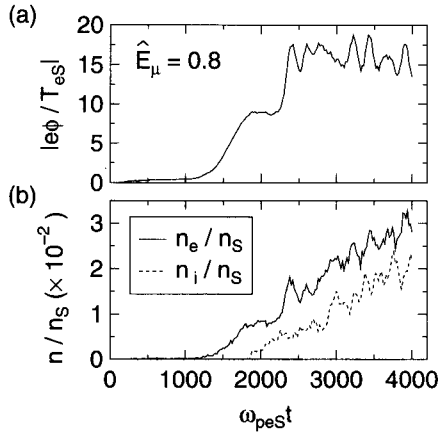


Fig. 5 Temporal evolutions of (a) the absolute value of potential drop $|e\phi/T_{es}|$ and (b) the density n/n_s at $x/\lambda_{DeS} = 128$, $y/\lambda_{DeS} = 64$ with $R_m^{-1} = 2.0$ for $\hat{E}_\mu = 0.8$.

connection with the electron dynamics.

4. Discussion

Let us mention a mechanism of the potential formation. In the case of the small wave amplitude ($\hat{E}_\mu = 0.2$), $|e\phi/T_{es}|$ starts to increase as soon as the plasma flow arrives at the ECR point ($\omega_{peS}t \approx 1200$), as already shown in the temporal evolution of $|e\phi/T_{es}|$, n_e , and n_i of Fig. 4. Since the large amount of electrons are accelerated by ECR and supplied to the downstream region at that time, n_e at $x/\lambda_{DeS} = 128$ extremely increases, causing the increase in $|e\phi/T_{es}|$. When ions subsequently arrive at the observation point ($x/\lambda_{DeS} = 128$), $|e\phi/T_{es}|$ saturates because the excess of the negative charge density begins to be compensated by the positive ions. Here, $|e\phi/T_{es}|$ is approximately equivalent to the $\epsilon_{e\parallel}/T_{es}$ in the downstream region. In this sense the potential formation is due to the ambipolar diffusion mechanism.

In the case of the large wave amplitude ($\hat{E}_\mu = 0.8$), on the other hand, both $|e\phi/T_{es}|$ and n_e increase not only at $\omega_{peS}t \approx 1200$ but also at $\omega_{peS}t \approx 2200$ when the plasma flow arrives at the collector. Since most of electrons diffuse along the field lines with ions in the plasma flow, a large number of electrons are reflected by the sheath potential in front of the collector at $\omega_{peS}t \approx 2200$. These electrons are again reflected on the opposite side by the magnetic gradient, *i.e.*, a magnetic mirror effect. Thus, the electrons reflected by the sheath potential and the magnetic mirror are trapped in the downstream region, which cause the second increase in n_e and $|e\phi/T_{es}|$ as described above. The electron reflection at the

magnetic mirror is enhanced with an increase in \hat{E}_μ , because the electrons can not pass through the mirror field due to the strong $-\mu\nabla_{\parallel}B$ force with large μ in the case of large \hat{E}_μ . Thus, $|e\phi/T_{es}|$ continues to increase due to the trapped electrons even though $\epsilon_{e\parallel}/T_{es}$ decreases with an increase in \hat{E}_μ .

5. Conclusion

The plasma potential formation under the configuration of diverging magnetic field is investigated by using a two-and-a-half dimensional particle simulation. The potential structure equivalent to the experimental result which has been demonstrated is confirmed to be observed. The absolute value of the potential drop in the downstream region from the ECR point increases depending on the wave amplitude E_μ . In the case of the small E_μ , the potential drop is generated as an ambipolar diffusion process, the value of which corresponds to the parallel electron energy $\epsilon_{e\parallel}$. In the case of the large E_μ , on the other hand, it is found that $|e\phi/T_{es}|$ more increases due to the electrons trapped in the downstream region between the magnetic mirror and the sheath potential in front of the collector. Thus, it is possible to generate the potential structure which efficiently accelerates ions without the requirement for high $\epsilon_{e\parallel}$.

Acknowledgment

The computations were performed at the Computer Center of Tohoku University and at the Advanced Computing System for Complexity Simulation at the National Institute for Fusion Science.

References

- [1] H.G. Kosmahl, D.B. Miller and G.W. Bathke, *J. Appl. Phys.* **38**, 4576 (1967).
- [2] W. Cronrath, N. Mayumi, M.D. Bowden, *et al.*, *J. Appl. Phys.* **82**, 1036 (1997).
- [3] Y. Okuno, Y. Ohtsu and H. Fujita, *J. Appl. Phys.* **74**, 5990 (1993).
- [4] G. Lu, P.H. Reiff, T.E. Moore, *et al.*, *J. Geophys. Res.* **97**, 16855 (1992).
- [5] T. Ohkawa, *Kakuyugo Kenkyu* **64**, 305 (1990).
- [6] R. Geller, N. Hopfgarten, B. Jacquot, *et al.*, *J. Plasma Phys.* **12**, 467 (1974).
- [7] T. Kaneko, R. Hatakeyama and N. Sato, *IEEE Trans. Plasma Sci.* **28**, 1747 (2000).
- [8] E.B. Hooper, Jr., *Phys. Plasmas* **2**, 4563 (1995).
- [9] S. Ishiguro, Y. Kishi and N. Sato, *Phys. Plasmas* **2**, 3271 (1995).